

## Triaxial shapes in the interacting boson model

K. Heyde, P. Van Isacker, M. Waroquier, and J. Moreau

*Institute for Nuclear Physics, B-9000 Gent, Belgium*

(Received 12 August 1983)

We suggest the use of cubic terms in the interacting boson model. It is shown that, examining the classical limit, such cubic terms can give rise to stable, triaxial shapes. Energy spectra are studied in the U(5), O(6), and SU(3) limits. Also, a more realistic case is studied in  $^{104}\text{Ru}$ .

Since the work of Wilets and Jean<sup>1</sup> and of Davydov, Filippov, and Chaban,<sup>2,3</sup> it is known that the  $\gamma$  degree of freedom plays an important role in many nuclei of the mass table where static (quadrupole) deformation occurs. These models adopt a geometrical picture of the nucleus to describe its collective excitations, as put forward by Bohr and Mottelson,<sup>4</sup> and emphasize the importance of deviations from axial symmetry. In the model of Jean and Wilets<sup>1</sup> the potential energy is assumed to be independent of the  $\gamma$  degree of freedom, hence the name  $\gamma$ -unstable rotor. In the model of Davydov *et al.*,<sup>2,3</sup> on the other hand, one proposes a rigid triaxial shape for the nucleus. More recently, similar calculations were carried out by Toki and Faessler.<sup>5</sup> Although these models are, in general, successful in reproducing the experimental data, they have as a disadvantage the lack of a unified theory, since each of these models is based on a different hypothesis concerning triaxiality.

The interacting boson model (IBM) of Arima and Iachello<sup>6</sup> has provided us with an alternative description of nuclear collective excitations, which in contrast to the geometrical models, is of an algebraic nature. One of the most attractive features of the IBM is certainly its unifying capacity and one might try to use this property to establish a coherent theory of triaxiality in the framework of the IBM. However, with the work of Ginocchio and Kirson<sup>7</sup> and, simultaneously, Dieperink *et al.*,<sup>8</sup> that bridged the gap between geometrical models of nuclear collective motion and the IBM, it became clear that even the most general Hamiltonian of the model in its original formulation of Ref. 6 cannot give rise to a stable, triaxial shape for the nucleus.

In this paper, we show that by incorporating cubic terms in the Hamiltonian of the IBM, one may obtain a stable, triaxially shaped nucleus and study the influence of such terms on the energy spectrum in each of the three dynamic symmetries. Our analysis will be completely restricted to the IBM-1, that is, making no distinction between protons and neutrons. This is in contrast to the re-

cent work of Dieperink and Bijker,<sup>9,10</sup> who showed that triaxiality also occurs in particular dynamic symmetries of the IBM-2 that does distinguish between protons and neutrons.

The Hamiltonian we consider is of the form

$$H = H_{sd} + \sum_L \theta_L [d^\dagger d^\dagger d^\dagger]^{(L)} \cdot [\tilde{d} \tilde{d} \tilde{d}]^{(L)}, \quad (1)$$

where  $H_{sd}$  is the standard Hamiltonian of the IBM,<sup>11,12</sup>

$$H_{sd} = \epsilon_d n_d + \kappa Q \cdot Q + \kappa' L \cdot L + \kappa'' P^\dagger \cdot P + q_3 T_3 \cdot T_3 + q_4 T_4 \cdot T_4. \quad (2)$$

We have studied for each of the three limits of the IBM-1 [U(5), O(6), and SU(3)] the influence of the various cubic terms of Eq. (1) on the energy spectrum. From our calculations it becomes clear that only the  $L=3$  term can induce stable triaxial shapes. In Figs. 1(a)–(c) we show typical spectra in the three limits. The parameters of Eqs. (1) and (2) are specified in the caption. Figures 1(a)–(c) illustrate that in the U(5) and O(6) limits both the ground-state band (g.s.b) and the first excited  $2^+$  band are not changed by the inclusion of cubic terms in the Hamiltonian. On the other hand, the  $3^+, 4^+, 5^+, \dots$ , bands are lowered in energy since for these levels the cubic term with  $L=3$  can give a diagonal energy contribution. In the SU(3) limit the ground-state band and the  $\beta$  band are unaltered but the  $\gamma$  band is shifted in energy with respect to the standard SU(3) calculation. These results clearly point out that, in the new Hamiltonian, the  $\gamma$  degree of freedom no longer is unstable but prefers a particular triaxial shape with  $\gamma \neq 0^\circ$  or  $60^\circ$ .

In order to obtain a more intuitive insight into the problem of triaxial shapes, the classical limit of the Hamiltonian of Eq. (1) can be calculated. In the intrinsic frame of reference one obtains a potential energy surface dependent on  $\beta$  and  $\gamma$ , which for a Hamiltonian with a  $L=3$  cubic term reads<sup>7,8,13</sup>

$$E(\beta, \gamma) = \epsilon_d \frac{N\beta^2}{1+\beta^2} + \kappa \left[ \frac{N}{1+\beta^2} \left( 5 + \frac{11}{4}\beta^2 \right) + \frac{N(N-1)}{(1+\beta^2)^2} \left[ \frac{\beta^4}{2} + 2\sqrt{2}\beta^3 \cos 3\gamma + 4\beta^2 \right] \right] + \kappa' \frac{6N\beta^2}{1+\beta^2} + \kappa'' \frac{N(N-1)}{4} \left[ \frac{1-\beta^2}{1+\beta^2} \right]^2 + q_3 N \frac{7}{5} \frac{\beta^2}{1+\beta^2} + q_4 \left[ N \frac{9}{5} \frac{\beta^2}{1+\beta^2} + N(N-1) \frac{18}{35} \frac{\beta^4}{(1+\beta^2)^2} \right] + \theta_3 N(N-1)(N-2) \frac{1}{7} \frac{\beta^6}{(1+\beta^3)^2} (-1 + \cos^2 3\gamma). \quad (3)$$

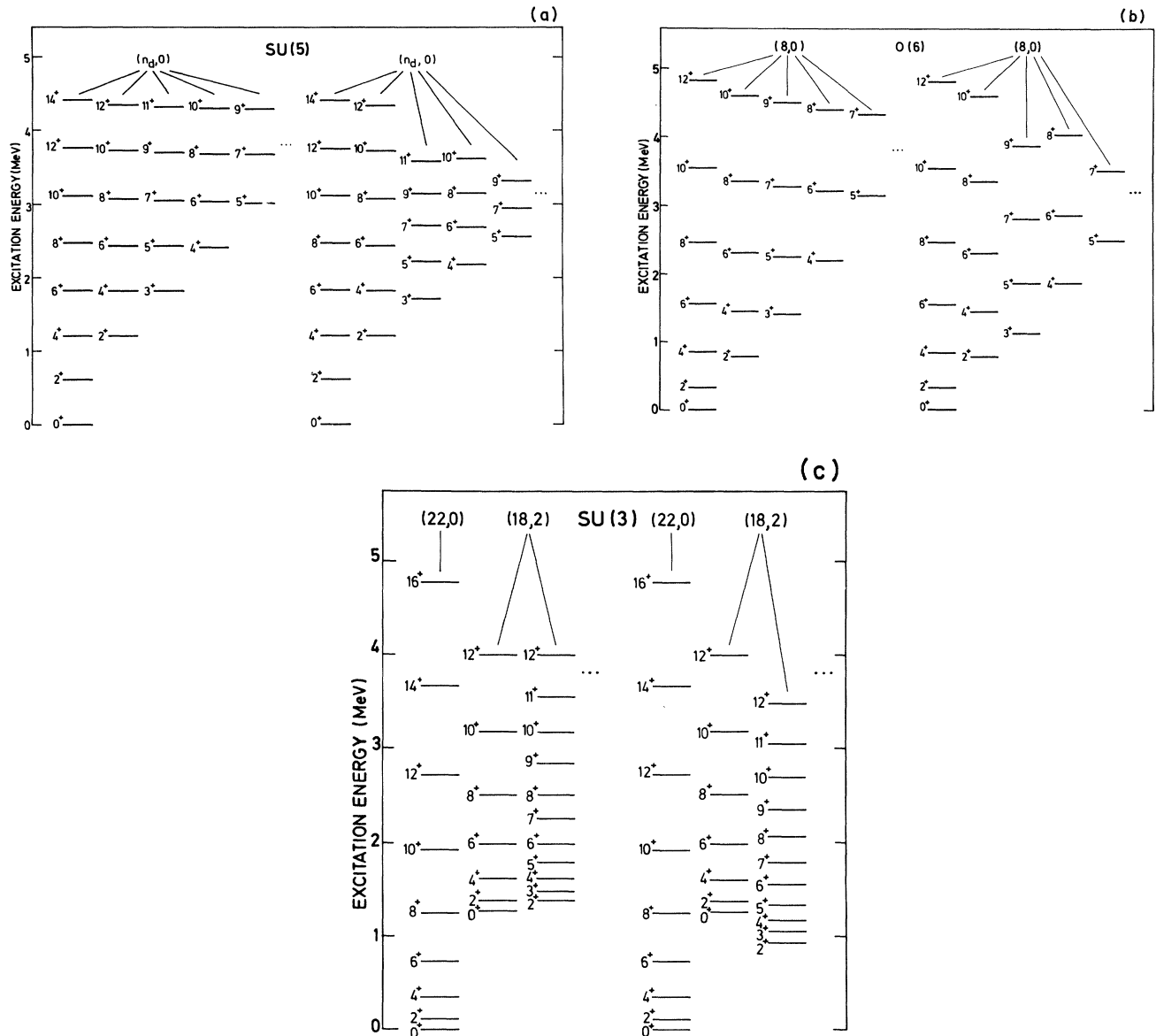


FIG. 1. (a) The lower band members in the U(5) limit for  $N=7$  bosons. The left part of the figure shows the spectrum in the exact U(5) limit and the right part shows the spectrum when the  $L=3$  cubic term is added. The parameters of Eqs. (1) and (2) are the following:  $\epsilon_d=0.6$  MeV,  $\kappa'=0.001$  MeV, and  $\theta_3=0.06$  MeV. (b) Same caption as (a), but for the O(6) limit with  $N=8$  bosons. The parameters of Eqs. (1) and (2) are the following:  $\kappa'=0.02$  MeV,  $\kappa''=0.1$  MeV,  $q_3=0.15$  MeV, and  $\theta_3=0.06$  MeV. (c) Same caption as (a), but for the SU(3) limit with  $N=11$  bosons. The parameters of Eqs. (1) and (2) are the following:  $\kappa=-0.02$  MeV,  $\kappa'=0.01$  MeV, and  $\theta_3=0.02$  MeV.

This expression allows us to visualize the influence of the  $L=3$  cubic term in a  $(\beta, \gamma)$  potential energy plot, as is illustrated in Figs. 2(a)–(c) in the case of the U(5), O(6), and SU(3) limits, respectively. One indeed observes that, in particular in the O(6) limit, a stable triaxial minimum results at  $\gamma=30^\circ$  and  $\beta \simeq 0.7$ . The need for cubic terms to have a minimum in  $E(\beta, \gamma)$ , different from  $\gamma=0^\circ$  or  $30^\circ$ , is clear. Without the cubic terms, the only dependence on  $\gamma$  in Eq. (3) resides in the  $\cos^3\gamma$  term, which always implies either a prolate or an oblate minimum (provided  $\kappa$  is negative), depending on the sign one considers in the quadrupole operator  $Q$ . Only by including terms propor-

tional to  $\cos^2 3\gamma$  does a stable, triaxial shape eventually arise. As studied by Van Isacker and Chen,<sup>13</sup> the cubic anharmonicities indeed induce such terms.

The above discussion is based upon a study of the minimum values  $(\beta, \gamma)$  of the expression  $E(\beta, \gamma)$  of Eq. (3) corresponding with a given IBM-1 Hamiltonian. Thereby, one concentrates on the *static* (potential energy) part of the Hamiltonian. In the full quantum mechanical problem, *dynamics* (kinetic energy) has to be taken into account properly which implies deviations from the minimum  $\gamma$  value. In this way, an *effective*  $\gamma$  value can be determined as the expectation value of  $\gamma$  using the quantum mechani-

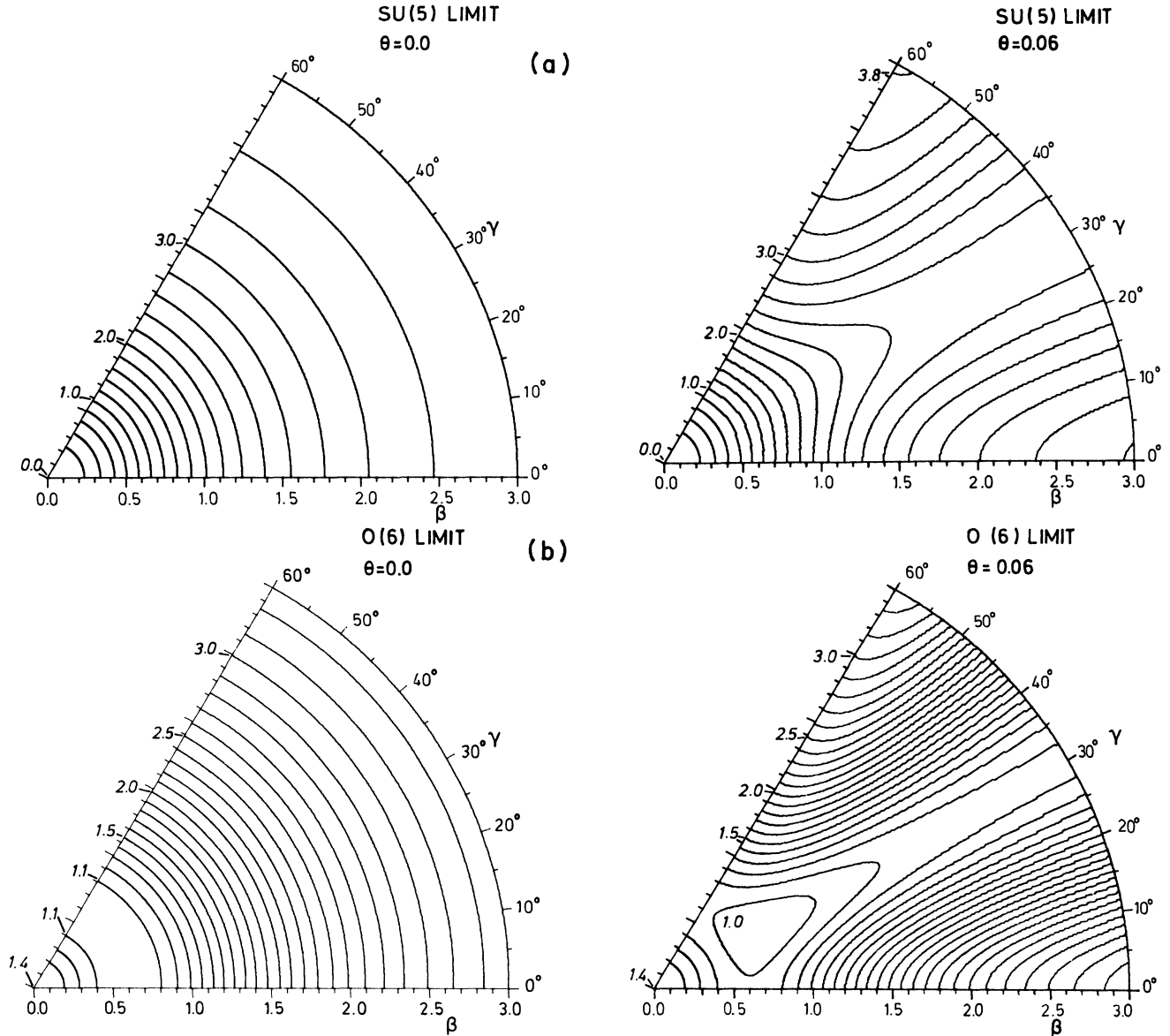


FIG. 2. (a) Potential energy surface, according to Eq. (3), for the U(5) limit with the parameters given in the caption of Fig. 1(a). (b) Potential energy surface, according to Eq. (3), for the O(6) limit with the parameters given in the caption of Fig. 1(b). (c) Potential energy surface, according to Eq. (3), for the SU(3) limit with the parameters given in the caption of Fig. 1(c).

cal wave function. Work in this direction is in progress.<sup>14,15</sup>

Recently, the nucleus  $^{104}\text{Ru}$  has been studied in the framework of the IBM.<sup>12,16</sup> The hexadecapole degree of freedom ( $g$  boson) was shown to be of crucial importance for the description of many detailed properties of this transitional nucleus. However, the excitation energies of the levels of the  $\gamma$  band are not substantially altered by the addition of a  $g$  boson and they strongly deviate from the experimental data (see Fig. 3). The fact that many of the experimental observations support the hypothesis of  $^{104}\text{Ru}$  being a triaxial nucleus<sup>16</sup> suggests the use of the  $L=3$  cubic term in the IBM Hamiltonian. Its effect is illustrated in Figs. 3 and 4. The levels of the  $\gamma$  band are changed from a  $(3^+, 4^+)$ ,  $(5^+, 6^+)$ , and  $(7^+, 8^+)$  odd-even sequence

into a band with more regular spacings, which is typical for a nucleus which is not  $\gamma$  soft or rigid triaxial, but has a shape somewhere in between. This example illustrates that the use of cubic terms in the IBM enables one to describe nuclei ranging from  $\gamma$  soft to rigid triaxial, hence covering a wide class of nuclei in the mass table.

We also have studied the g.s.b.  $B(E2; I \rightarrow I-2)$  values and the diagonal reduced matrix elements  $\langle I || T(E2) || I \rangle$ , using the standard IBM-1 electric quadrupole operator, i.e.,

$$T(E2) = e_{ds}(d^\dagger s + s^\dagger \tilde{d})^{(2)} + e_{dd}(d^\dagger \tilde{d})^{(2)}. \quad (4)$$

Conforming to the calculation of Ref. 12, we use the effective boson charges  $e_{ds} = 0.1 e b$  and  $e_{dd} = -0.05 e b$ . In Tables I and II, we compare the calculated quantities with

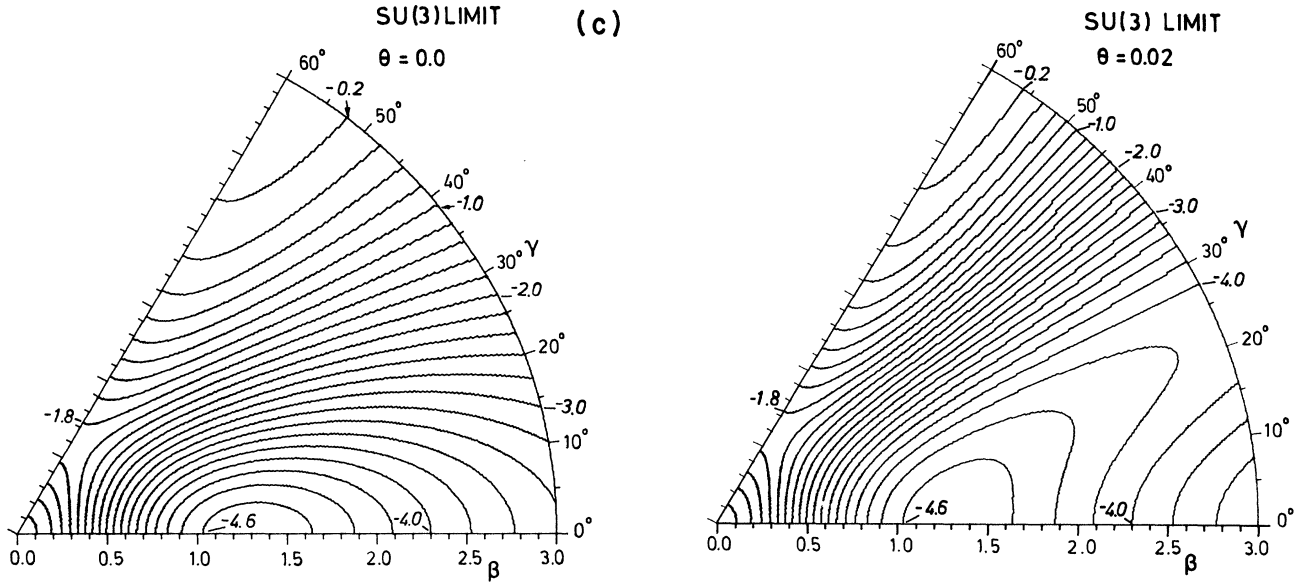


FIG. 2. (Continued.)

the most recent experimental data of Stachel *et al.* (Refs. 16 and 17). The calculated  $B(E2; I \rightarrow I-2)$  and  $\langle I || T(E2) || I \rangle$  quantities, when including the cubic anharmonicities in the Hamiltonian of Eq. (1), are almost equal to the results of the standard IBM-1 calculation. Also, the theoretical  $B(E2; I \rightarrow I-2)$  values are not as large as the experimental  $6^+ \rightarrow 4^+$ ,  $8^+ \rightarrow 6^+$ , and  $10^+ \rightarrow 8^+$   $B(E2)$  values. The quadrupole moments show a smooth growing

trend (in absolute value) with increasing spin, whereas the experimental numbers show a more constant behavior as a function of angular momentum, at least up to spin  $I^\pi = 6^+$ .

Some of the shortcomings probably originate from the fact that, when including cubic terms in the Hamiltonian, one should at the same time extend the  $E2$  operator to higher order, i.e.,

$$T(E2) = e_{ds}(d^\dagger s + s^\dagger \tilde{d})^{(2)} + e_{dd}(d^\dagger \tilde{d})^{(2)} + \sum_{L=\text{even}} e_L \{ [(d^\dagger d^\dagger)^{(L)} (\tilde{d} \tilde{s})^{(2)}]^{(2)} + \text{H.c.} \} + \sum_{\substack{L, L' \\ \text{even}}} e_{L, L'} [(d^\dagger d^\dagger)^{(L)} (\tilde{d} \tilde{d})^{(L')}]^{(2)}. \quad (5)$$

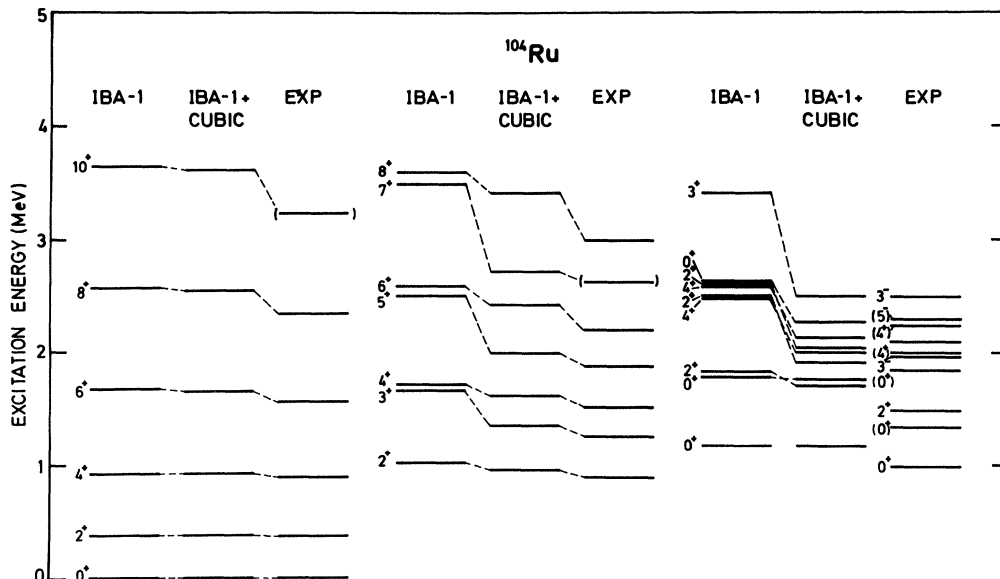


FIG. 3. Comparison of the experimental spectrum of  $^{104}\text{Ru}$  (from Ref. 16) with a IBM-1 calculation ( $\epsilon_d = 0.6$  MeV,  $\kappa = -0.01$  MeV,  $\kappa' = 0.01$  MeV,  $\kappa'' = 0.098$  MeV, and  $q_3 = 0.05$  MeV), and with a IBM-1 calculation with the same parameters and a  $L=3$  cubic term ( $\theta_3 = 0.11$  MeV).

TABLE I. The ground-state band  $B(E2; I \rightarrow I-2)$  values in units of  $e^2 b^2$ .

$I \rightarrow I-2$	Expt <sup>a</sup>	IBM-1 <sup>b</sup>	
		$\theta_3=0$	$\theta_3=0.11$
2→0	0.165	0.168	0.168
4→2	0.239(26)	0.246	0.246
6→4	0.335(28)	0.273	0.275
8→6	0.364(25)	0.272	0.276
10→8	0.332(7)	0.250	0.254
12→10	0.224( $^{+121}_{-106}$ )	0.211	0.213
14→12		0.155	0.156

<sup>a</sup>From Stachel *et al.* (Refs. 16 and 17).

<sup>b</sup>Parameters given in the caption of Fig. 3.

This is still not the most general one- and two-body transition operator for  $s$  and  $d$  bosons. We will later indicate with arguments based on perturbation theory that the operator (5) is appropriate for describing g.s.b.  $E2$  properties (see Fig. 8). The extension (5) has the disadvantage of increasing the number of effective boson charges significantly. One can show that in the pure U(5) limit the calculation of g.s.b.  $B(E2)$  values and diagonal reduced matrix elements needs only *two* of these effective boson charges.

In the U(5) limit the g.s.b. wave functions read

$$|s^N; 0^+\rangle, |s^{N-1}d; 2^+\rangle, |s^{N-2}d^2; 4^+\rangle, |s^{N-3}d^3; 6^+\rangle, \dots, \quad (6)$$

and the extra contributions to  $B(E2; I \rightarrow I-2)$  and  $\langle I || T(E2) || I \rangle$  become

$$B(E2; I \rightarrow I-2) = (N - n_d)(n_d + 1) \left[ e_{ds} + e_4 \frac{\sqrt{5}}{3} n_d \right]^2 \quad (7)$$

(only  $L=4$  contributes), and

$$\langle I || T(E2) || I \rangle = \left[ \frac{(2I+1)(2I+3)(2I+2)}{7I(2I-1)} \right]^{1/2} [e_{dd}n_d + e_{4,4} \frac{7}{3} \sqrt{2/11}(n_d-1)n_d] \quad (8)$$

(only  $L=L'=4$  contributes), respectively.

In Figs. 5 and 6 we show  $B(E2; I \rightarrow I-2)$  and  $\langle I || T(E2) || I \rangle$  as a function of  $I$  in the U(5) limit for  $N=8$ . Since the higher order terms in the electric quadrupole operator of Eq. (5) will generally be of the order

$$e_L \simeq e_{L,L'} \simeq e_1^2 \text{ body},$$

we use in the schematic U(5) calculations the values  $e_4=0.01$  e b and  $e_{4,4}=0.01$  e b. The g.s.b.  $B(E2; I \rightarrow I-2)$  values grow to much larger values for the  $6^+ \rightarrow 4^+$ ,  $8^+ \rightarrow 6^+$ , and  $10^+ \rightarrow 8^+$  transitions, and the diagonal reduced  $E2$  matrix elements no longer show the pure U(5) behavior. Both facts do show up in the  $^{104}\text{Ru}$  nucleus,<sup>16,17</sup> a nucleus that seems to be situated in a transitional region between the U(5) and O(6) limits.<sup>18</sup>

If one studies more complicated situations [other than U(5)] and other  $E2$  transitions, the above simplifications for the U(5) limit are not valid any more. One way out is to introduce cubic anharmonicities in a consistent-Q

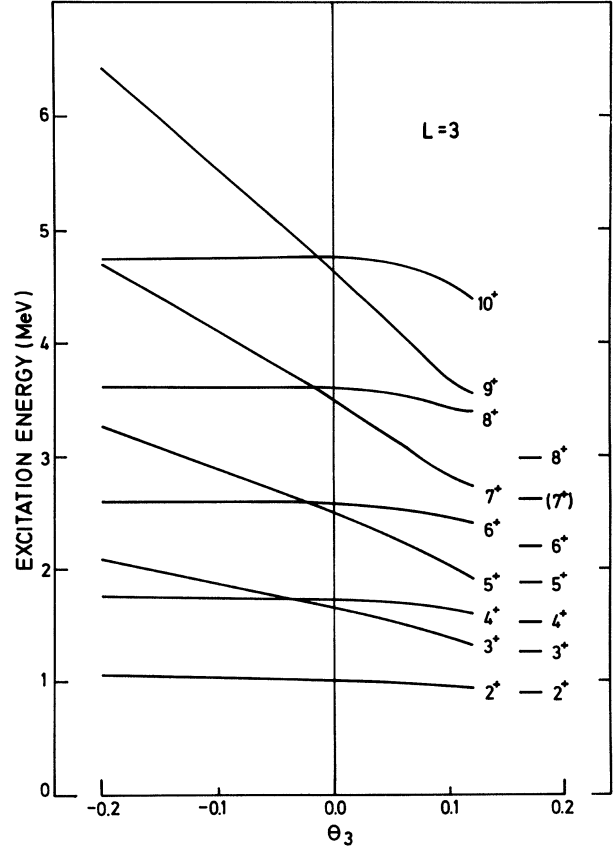


FIG. 4. Variation of the levels of the  $\gamma$  band as a function of the strength parameter  $\theta_3$ . The parameters of the IBM-1 Hamiltonian of Eqs. (1) and (2) are given in the caption of Fig. 3. At the extreme right, the experimental  $\gamma$  band in  $^{104}\text{Ru}$  is also drawn for comparison.

framework, as discussed by Warner and Casten,<sup>19,20</sup> where the Hamiltonian

TABLE II. Diagonal reduced matrix elements  $\langle I || T(E2) || I \rangle$  in the ground-state band in units of  $e$  b.

$I$	Expt <sup>a</sup>	IBM-1 <sup>b</sup>	
		$\theta_3=0$	$\theta_3=0.11$
2	-0.91(40)	-0.75	-0.75
4	-0.42(31)	-0.91	-0.87
6	-0.54(22)	-1.03	-0.95
8	-0.76(31)	-1.11	-1.03
10		-1.18	-1.11
12		-1.24	-1.19
14		-1.29	-1.29

<sup>a</sup>From Stachel *et al.* (Refs. 16 and 17).

<sup>b</sup>Parameters given in the caption of Fig. 3.

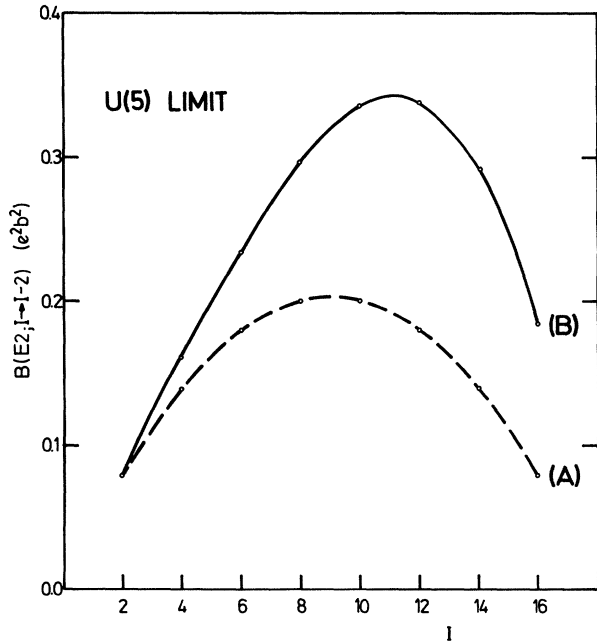


FIG. 5. Schematic model calculation in the U(5) limit for the g.s.b.  $B(E2; I \rightarrow I - 2)$  values, if one includes two-body boson transition operators in the  $T(E2)$  operator [see Eq. (5)]. The expression is drawn for  $e_{ds} = 0.1 e b$  and for both  $e_4 = 0 e b$  (A) and  $e_4 = 0.01 e b$  (B).

$$H = \kappa Q \cdot Q + \kappa' L \cdot L \quad (9)$$

is used, now with an extended quadrupole operator as given in Eq. (5) [ $T(E2) = e_{ds} Q$ ], but using the same parameters for the quadrupole operator in both the Hamiltonian and the  $E2$  transition operator. Thereby the number of parameters is reduced significantly.

As a final point, we show that a cubic interaction can be obtained as a renormalized interaction within the  $sd$ -

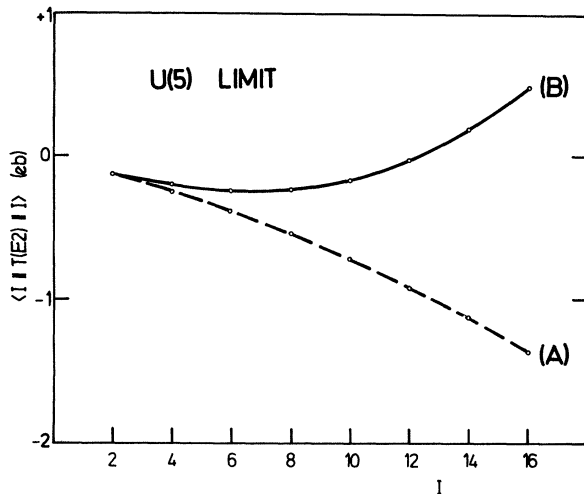


FIG. 6. Schematic model calculation in the U(5) limit for the g.s.b. diagonal reduced matrix element  $\langle I || T(E2) || I \rangle$  if one includes two-body transition operators in the  $T(E2)$  operator [see Eq. (5)]. The expression is drawn for  $e_{dd} = -0.05 e b$  and for both  $e_{4,4} = 0 e b$  (A) and  $e_{4,4} = 0.01 e b$  (B)

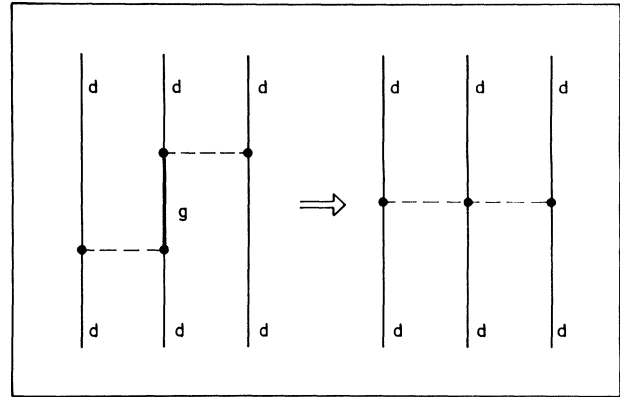


FIG. 7. Diagrammatic representation of the energy correction (in second order perturbation theory) to the  $|s^{N-3}d^3\rangle$  configuration using a quadrupole-quadrupole interaction (left) and the corresponding effective three-body interaction after the exclusion of the  $g$  boson from the model space (right).

boson space, due to the exclusion of the higher angular momentum bosons. The most important one of these bosons is the  $g$  boson which is useful in describing many features of transitional nuclei.<sup>12,21-24</sup> With a  $g$  boson, the one-body quadrupole operator becomes

$$Q = (d^\dagger s + s^\dagger \tilde{d})^{(2)} + \alpha (d^\dagger \tilde{d})^{(2)} + \beta (d^\dagger \tilde{g} + g^\dagger \tilde{d})^{(2)} + \gamma (g^\dagger \tilde{g})^{(2)} \\ \equiv Q_{sd} + \beta Q_{gd} + \gamma Q_{gg} \quad (10)$$

The correction to the energy of the  $|s^{N-3}d^3\rangle$  contributions in second order perturbation theory, using as a residual interaction a quadrupole-quadrupole force  $\kappa Q \cdot Q$ , can be written as (see Fig. 7)

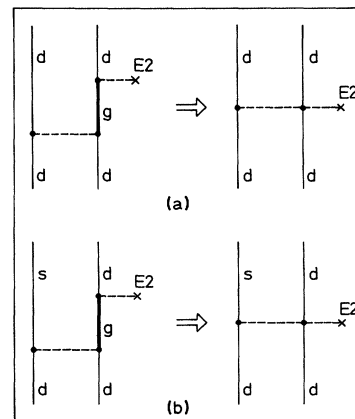


FIG. 8. Diagrammatic representation of the correction (in lowest order perturbation theory) to the  $T(E2)$  operator of Eq. (4) using a quadrupole-quadrupole interaction and a  $g$  boson as an intermediate state for the diagonal (a) and the  $I \rightarrow I - 2$  (b) g.s.b.  $E2$  matrix elements. The corresponding matrix elements of the effective two-boson transition operator, when excluding the  $g$  boson from the model space, are given on the right-hand side.

$$\begin{aligned}
\delta E(d^3) &= \kappa^2 \frac{\alpha^2 \beta^2}{\Delta E} \left| \langle s^{N-3} d^3 | (d^\dagger \tilde{d})^{(2)} \cdot Q_{gd} | s^{N-2} d^2 g \rangle \right|^2, \\
&= \kappa^2 \frac{\alpha^2 \beta^2}{\Delta E} \langle s^{N-3} d^2 | (d^\dagger \tilde{d})^{(2)} \cdot (d^\dagger \tilde{d})^{(2)} | s^{N-3} d^2 \rangle \langle d | Q_{gd} \cdot Q_{gd} | d \rangle \\
&= \kappa^2 \frac{\alpha^2 \beta^2}{\Delta E} \langle s^{N-3} d^3 | (d^\dagger \tilde{d})^{(2)} \cdot (d^\dagger \tilde{d})^{(2)} n_d | s^{N-3} d^3 \rangle. \tag{11}
\end{aligned}$$

Thus, the renormalized effective interaction becomes

$$H_{\text{eff}} = \kappa^2 \frac{\alpha^2 \beta^2}{\Delta E} (d^\dagger \tilde{d})^{(2)} \cdot (d^\dagger \tilde{d})^{(2)} n_d, \tag{12}$$

where  $\Delta E = \epsilon_d - \epsilon_g$  and  $n_d$  is the  $d$ -boson number operator. By recoupling the angular momenta, the effective interaction can be rewritten as

$$H_{\text{eff}} = \kappa^2 \frac{\alpha^2 \beta^2}{\Delta E} \sum_L \theta_L [d^\dagger d^\dagger d^\dagger]^{(L)} \cdot [\tilde{d} \tilde{d} \tilde{d}]^{(L)}, \tag{13}$$

which indeed is a three-body interaction between the  $d$  bosons, resulting from *excluding* the  $g$  boson from the model space.

Similarly, an effective boson  $E2$  operator can be obtained by excluding the  $g$  boson from the model space. Using lowest order perturbation theory, the higher order corrections to the  $E2$  operator can be obtained from the diagrams of Figs. 8(a) and (b), for the diagonal reduced  $E2$  matrix element  $\langle I || T(E2) || I \rangle$ , and the g.s.b  $B(E2; I \rightarrow I-2)$  value, respectively. These diagrams correspond to

$$\langle s^{N-n_d} d^{n_d} || e_{sd} Q || s^{N-n_d} d^{n_d-1} g \rangle \langle s^{N-n_d} d^{n_d-1} g | \kappa Q \cdot Q | s^{N-n_d} d^{n_d} \rangle \frac{1}{\Delta E_1}, \tag{14a}$$

and

$$\langle s^{N-n_d+1} d^{n_d-1} || e_{sd} Q || s^{N-n_d+1} d^{n_d-2} g \rangle \langle s^{N-n_d+1} d^{n_d-2} g | \kappa Q \cdot Q | s^{N-n_d} d^{n_d} \rangle \frac{1}{\Delta E_2}, \tag{14b}$$

where  $\Delta E_1 = \epsilon_d - \epsilon_g$  and  $\Delta E_2 = 2\epsilon_d - \epsilon_s - \epsilon_g$ . Using as the interaction Hamiltonian the quadrupole-quadrupole force  $\kappa Q \cdot Q$ , with the extended quadrupole operator of Eq. (10), the renormalized effective  $E2$  operator becomes, after some Racah algebra,

$$\delta T(E2) = e_{sd} \alpha \beta^2 \frac{\kappa}{\Delta E_1} [(d^\dagger d^\dagger)^{(4)} (\tilde{d} \tilde{d})^{(4)}]^{(2)}, \tag{15a}$$

and

$$\delta T(E2) = e_{sd} \beta^2 \frac{\kappa}{\Delta E_2} [(s^\dagger d^\dagger)^{(2)} (\tilde{d} \tilde{d})^{(4)}]^{(2)} + \text{H.c.}, \tag{15b}$$

corresponding to the expressions (14a) and (14b), respectively.

These effective two-boson transition operators are shown on the right-hand side in Figs. 8(a) and (b). The vertex now affects *two* bosons in the  $E2$  transition. The magnitude of these higher order terms could in principle be calculated from the knowledge of  $\alpha$ ,  $\beta$ ,  $\kappa$ , and the energy denominators  $\Delta E_1$  and  $\Delta E_2$ . Using the values from Ref. 12, one obtains the order of magnitude of the effective two-boson transition operator as  $\sim 0.01$  e b.

In conclusion, we have shown that nuclei with triaxial features can be described in the framework of the IBM by considering cubic terms in the model Hamiltonian. The effect of this addition to the Hamiltonian was studied in the three different limits of the IBM and visualized by taking the classical limit of this extended Hamiltonian. This study pointed out clearly the occurrence of a stable, triaxial minimum if one considers the  $L=3$  cubic term. As an illustration of the usefulness of this approach, we presented an application to the triaxial nucleus  $^{104}\text{Ru}$ . With regards to electromagnetic properties of the ground-state band, we showed that these are not changed drastically by cubic terms in the IBM-1, unless these higher order terms are treated consistently in Hamiltonian *and* transition operators. Finally, we indicated that such cubic terms result as an effective interaction in the  $sd$ -boson model space, as a result of excluding higher angular momentum bosons from the model space.

The authors are most grateful to F. Iachello, R. Casten, and J. Stachel for many discussions. They are indebted to the IKW (Interuniversitair Instituut Kernwetenschappen) for financial support. Three of the authors (P.V.I., M.W., and J.M.) acknowledge the NFWO (Nationaal Fonds voor Wetenschappelijk Onderzoek) for financial support.

- <sup>1</sup>L. Wilets and M. Jean, *Phys. Rev.* **102**, 788 (1956).
- <sup>2</sup>A. S. Davydov and G. F. Filippov, *Nucl. Phys.* **8**, 237 (1958).
- <sup>3</sup>A. S. Davydov and A. A. Chaban, *Nucl. Phys.* **20**, 499 (1960).
- <sup>4</sup>A. Bohr, *K. Dan. Vidensk. Selsk. Mat.-Fys. Medd.* **26**, No. 14 (1952); A. Bohr and B. R. Mottelson, *ibid.* **27**, No. 16 (1953).
- <sup>5</sup>H. Toki and A. Faessler, *Z. Phys. A* **276**, 35 (1976).
- <sup>6</sup>A. Arima and F. Iachello, *Ann. Phys. (N.Y.)* **99**, 253 (1976); **111**, 201 (1978); **123**, 468 (1979).
- <sup>7</sup>J. N. Ginocchio and M. W. Kirson, *Phys. Rev. Lett.* **44**, 1744 (1980); *Nucl. Phys.* **A350**, 31 (1980).
- <sup>8</sup>A. E. L. Dieperink, O. Scholten, and F. Iachello, *Phys. Rev. Lett.* **44**, 1747 (1980).
- <sup>9</sup>A. E. L. Dieperink and R. Bijker, *Phys. Lett.* **116B**, 77 (1982).
- <sup>10</sup>A. E. L. Dieperink, in *Progress in Particle and Nuclear Physics*, edited by D. Wilkinson (Plenum, New York, 1983), Vol. 9, p. 121.
- <sup>11</sup>F. Iachello, in *Dronten Nuclear Structure Summer School*, edited by C. Abrahams, K. Allaart, and A. E. L. Dieperink (Plenum, New York, 1982), p. 53.
- <sup>12</sup>K. Heyde, P. Van Isacker, M. Waroquier, G. Wenes, Y. Gignase, and J. Stachel, *Nucl. Phys.* **A398**, 235 (1983).
- <sup>13</sup>P. Van Isacker and J. Q. Chen, *Phys. Rev. C* **24**, 684 (1981).
- <sup>14</sup>O. Castaños, A. Frank, and P. Van Isacker, *Phys. Rev. Lett.* (to be published).
- <sup>15</sup>R. F. Casten, A. Aprahamian, and D. D. Warner, *Phys. Rev. C* (unpublished).
- <sup>16</sup>J. Stachel, N. Kaffrell, E. Grosse, H. Emling, H. Folger, R. Kulesa, and D. Schwalm, *Nucl. Phys.* **A383**, 429 (1982).
- <sup>17</sup>J. Stachel *et al.*, Gesellschaft für Schwerionenforschung Report No. GSI-83-20, 1983.
- <sup>18</sup>J. Stachel, P. Van Isacker, and K. Heyde, *Phys. Rev. C* **25**, 650 (1982).
- <sup>19</sup>D. D. Warner and R. F. Casten, *Phys. Rev. Lett.* **48**, 1385 (1982).
- <sup>20</sup>D. D. Warner and R. F. Casten, *Phys. Rev. C* **25**, 2019 (1982).
- <sup>21</sup>P. Van Isacker, K. Heyde, M. Waroquier, and G. Wenes, *Nucl. Phys.* **A380**, 383 (1982).
- <sup>22</sup>O. Scholten, *Phys. Lett.* **114B**, 5 (1982).
- <sup>23</sup>K. A. Sage and B. R. Barrett, *Phys. Rev. C* **22**, 1705 (1980).
- <sup>24</sup>K. A. Sage, P. R. Goode, and B. R. Barrett, *Phys. Rev. C* **26**, 668 (1983).